A COMPARATIVE EVALUATION OF GEOREFERENCING TECHNIQUES IN UAV PHOTOGRAMMETRY: A CASE STUDY FROM THE CZECH REPUBLIC

Velile MOYO [1*], ***Michal KAČMAŘÍK*** [1]

DOI : 10.21163/GT_2025.202.13

ABSTRACT

The study evaluates the positional accuracy of geospatial products generated using direct (GNSS RTK-based) and indirect (Ground Control Points-based) georeferencing methods in UAV photogrammetry. Using the DJI Mavic 3 Enterprise quadcopter, surveys were conducted at two contrasting sites in the Czech Republic: a flat agricultural area and rugged terrain in the area affected by a landslide. Acquired RGB image sets were processed using consistent photogrammetric workflows. Resulting digital elevation models (DEMs) and orthophoto mosaics were analyzed against independently measured control points. Vertical and horizontal accuracies were assessed through RMSE and haversine-based distance calculations. Findings indicate that while both georeferencing methods produced centimeter-level accuracy, indirect georeferencing using GCPs yielded better quality in height. For horizontal accuracy, the results slightly varied between the two areas. In the flat area, direct georeferencing produced slightly better accuracy than indirect georeferencing whereas in the hilly area, the GCP-based approach was slightly superior. The study concludes that while GCPs can still provide some benefits in the quality of georeferencing, RTK-enabled UAVs offer a practical alternative for rapid, efficient deployment in suitable contexts.

Key-words: *UAV photogrammetry; Georeferencing; RTK; Digital Elevation Model; Orthomosaic*

1. INTRODUCTION

Unmanned Aerial Vehicles (UAVs) have quickly become a mature technology for capturing high quality spatial data with reasonable cost as shown e.g. by Colomina & Molina (2014), Gomez and Purdie (2016), Cromwell et al. (2021) or Mohsan et al. (2022). A set of properly acquired RGB images with sufficient overlaps in combination with their photogrammetric processing (Colomina et al., 2008) enable the production of detailed outputs such as digital elevation models (DEMs), 3D models or orthophoto mosaics. For practical use of these outputs, it is usually necessary to ensure their georeferencing to a selected spatial coordinate system. The standard solution is based on using a set of ground control points (GCPs) that are signaled in the area of interest at the time of image acquisition, and their position is accurately determined by some independent measurement technique. This approach is usually referred to as in-direct georeferencing. Since GCPs do not usually occur naturally in the selected area, they need to be manually positioned and collected again after the flight. This work, of course, adds significantly to the total time spent on data collection. If the imaging sensor or carrier used is equipped with its own localization unit, it is possible to use the information about the position of the device at the moment of image creation directly for georeferencing. This method is known as direct georeferencing. Localization units almost always rely on Global Navigation Satellite System (GNSS) technology, sometimes in combination with measurements from an Inertial Measurement Unit (IMU).

[1] *Department of Geoinformatics, Faculty of Mining and Geology, VŠB-Technical University of Ostrava, Czech Republic; velile.moyo.st@vsb.cz* [*], *michal.kacmarik@vsb.cz.*

Recently, the integration of Real-Time Kinematic (RTK) GNSS positioning technology into UAVs has begun. RTK is an advanced and widely used positioning technique based on differential measurements, typically achieving positioning accuracy within a few centimeters (Teunissen & Montenbruck, 2017). This represents a significant improvement in accuracy compared to common GNSS receivers that utilize the basic Standard Point Positioning (SPP) technique. Initially, only high-end devices were equipped with RTK GNSS receivers. The situation changed in year 2018 with announcement of the DJI Phantom 4 RTK quadcopter with a price below 6000 EUR (https://www.dji.com/newsroom/news/dji-launches-the-phantom-4-rtk-globally). Today, the market offers several comparable solutions at a similar cost.

Implementation of GNSS RTK technique in easily accessible UAVs has significantly advanced remote sensing applications, particularly in enhancing the accuracy of direct georeferencing. The comparative analysis of using RTK systems with traditional Ground Control Points (GCPs) has generated considerable interest in the remote sensing and photogrammetry communities, leading to new insights relevant to the accuracy of geospatial products. Recent studies such as Nakata et al. (2023) and Tomaštík et al. (2019) indicated that RTK-equipped UAVs can produce reliable geospatial datasets with reduced reliance on GCPs. Czyża et al. (2023) demonstrated advancements in UAV pose estimation accuracy due to RTK, suggesting that high-precision outputs can be achieved even without traditional GCPs. Both Nam-Bui et al. (2020) and Rauhala et al. (2023) discussed the use of RTK positioning over traditional GCPs for UAV-based topographic mapping. Nam-Bui et al. (2020) emphasized the importance of RTK in improving the accuracy of DEMs in complex open-pit mine environments, reducing reliance on GCP placement. Similarly, Rauhala et al. (2023) compared multiple UAV platforms and highlighted the advantages of RTK-enabled UAVs, such as the DJI Phantom 4 RTK, which significantly reduced georeferencing errors compared to traditional GCP-based methods.

The limitations associated with GCP-dependent methodologies have been analyzed in several studies. Štroner et al. (2021), highlighting the time and resource investments required for effective georeferencing. Stott et al. (2020) emphasized that while GCPs improve geometric accuracy, they complicate the operational logistics of UAV surveying, which can potentially compromise rapid response times in critical applications such as disaster management. However, several studies such as Atik & Arkali (2025) indicated that removing all GCPs can lead to significant errors, especially in regions with complex landforms and potential instability. Przybilla et al. (2020) noted that in certain contexts, particularly in variable or obstructed environments, maintaining a few GCPs can prevent accuracy deficits. Hence it is crucial to understand the variabilities in positional accuracy.

The performance of RTK in various environments presents unique challenges that necessitate careful examination. Nakata et al. (2023) explored microtopography changes due to soil erosion in agricultural landscapes using the UAV-RTK-PPK (Post-Processing Kinematic) method. Building on previous studies such as Przybilla et al. (2020), which primarily focused on flat or moderate terrain under favorable conditions, Elias et al. (2024) extended the application of RTK-based UAV photogrammetry to complex landscapes. Their findings demonstrate that high-accuracy 3D point clouds, with errors limited to a few centimeters, can be achieved even in challenging terrains by leveraging advanced image processing techniques, direct georeferencing, and optimized flight configurations, such as cross-grid and oblique imaging strategies.

Other factors contribute to the quality of data derived from UAVs which go alongside georeferencing techniques for example, the inclusion of oblique photographs. Martínez-Carricondo et al. (2023) conducted thorough accuracy assessments of RTK/PPK UAV-photogrammetry projects, highlighting that differential corrections from multiple GNSS fixed base stations significantly impact data quality. Their research aimed to enhance the accuracy of UAV photogrammetric projects by leveraging GNSS RTK receivers for direct georeferencing, eliminating the need for GCPs or oblique photographs. Szypuła (2024)'s findings indicated that the quality of elevation models derived from UAV measurements fluctuates based on the UAV equipment used and the terrain conditions. Szypuła (2024) discussed the improvement of accuracy for UAV-based DEMs without GCPs but implies that achieving optimal results often still relies on GCP methodologies in complex environments. This

perspective indicates that while RTK systems provide a valuable alternative, there remains a knowledge gap in understanding the accuracy thresholds across different applications and landscape complexities. The comparative accuracy using both methods across different terrains remains inadequately addressed.

This study systematically compares the accuracy of geospatial products generated using RTK (direct georeferencing) and non-RTK (in-direct georeferencing) datasets from the widespread quadcopter DJI Mavic 3 Enterprise in two contrasting areas in the Czech Republic. By evaluating both vertical and horizontal accuracies and by considering factors such as the influence of direct georeferencing versus traditional GCP deployment, this study aims to reconcile conflicting findings in previous studies and offer practical recommendations for UAV-based mapping. The findings can significantly contribute to this dialogue, addressing gaps related to the comparative performance of RTK/PPK based and GCPs based workflows in diverse landscapes.

2. METHODS AND MATERIALS

2.1. Study area

This study was conducted in two distinct areas of interest within the Czech Republic, each characterized by unique topographical and environmental features. The contrasting landscapes - one flat and agricultural, the other mountainous and landslide-prone, provide an ideal setting to assess and compare the accuracy of UAV products derived under direct and in-direct georeferencing setup.

Area 1 is situated in a flat, predominantly agricultural landscape near the city of Ostrava, Czech Republic (**Fig. 1**). The selected area covers about 4 ha where the range of altitudes is in the order of a few meters. At the time of data collection, the field was covered with low growing crops, with part of the area occupied by bare soil. The closest GNSS reference station is located at a short distance of 1.5 km. The relatively uniform terrain and close GNSS infrastructure offers a controlled environment for assessing UAV performance under optimal mapping conditions.

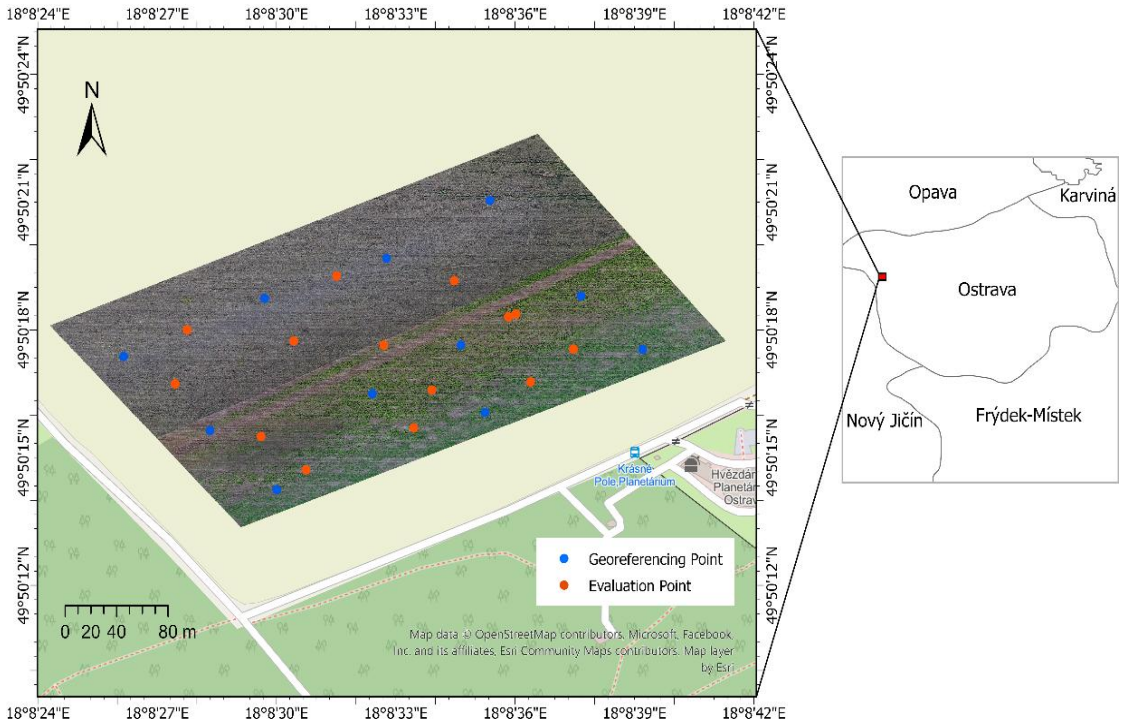

Fig. 1. Ostrava Area of Interest. Source of background map: Open Street Map.

In contrast, Girova (Area 2) is located in the Moravian-Silesian Region near the town Jablunkov in the Silesian Beskydy mountain range (**Fig. 2**). The selected area lies in the site of a large landslide which happened in May 2010. With its length of about 1.1 km and maximum width of 280 m, it has been one of the largest landslides in the Czech Republic in the last decades (Baroň et al., 2011). On the selected site of approximately 4 ha there is a very diverse terrain with a difference in elevation of about 40 m, parts of which are covered with bare land and others with different vegetation (mature forest, low forest, scrub). The complex topography and the whole environment make it an ideal testbed for evaluating the performance of UAV-derived DEMs and orthophoto mosaics under challenging conditions. The site is located close to the border with Slovakia and Poland, the nearest GNSS reference station is at a distance of 25 km.

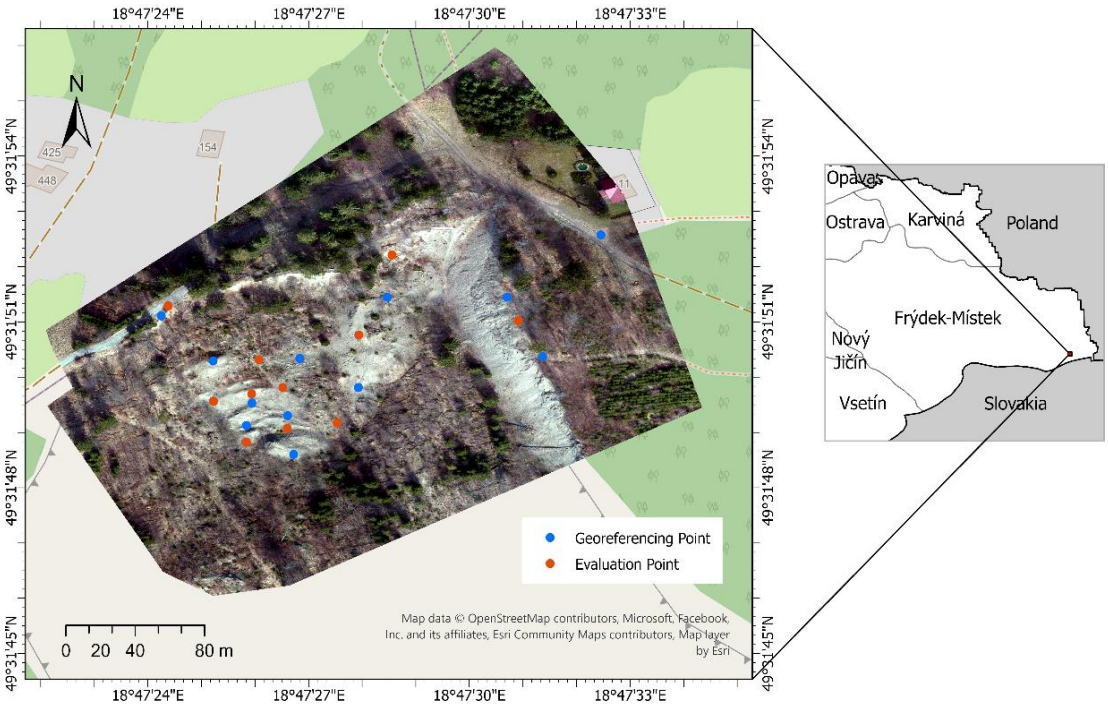

Fig. 2. Girova Area of Interest. Source of background map: Open Street Map.

Together, these two study areas allow for a robust comparison of UAV survey performance across different environmental settings, offering insights into the influence of terrain complexity and proximity of GNSS infrastructure for RTK positioning on the realized georeferencing approaches.

2.2. Data acquisition

Data collection was carried out using a DJI Mavic 3 Enterprise quadcopter equipped with an RGB sensor. This model is currently one of the most widely used drones for photogrammetric data acquisition. The main RGB camera of the DJI Mavic 3 Enterprise features a CMOS sensor with an effective resolution of 20 megapixels. The 4/3" sensor dimensions are approximately 17.3 × 13.0 mm, paired with a fixed lens that provides a 35-mm equivalent focal length of 24 mm. The camera also offers an adjustable aperture range from f/2.8 to f/11 (https://enterprise.dji.com/mavic-3-enterprise/specs). The UAV is equipped with a conventional GNSS receiver, relying on a basic SPP positioning technique. However, additional GNSS RTK module can be mounted on the UAV which offers accurate RTK positioning. Its performance was tested in this work. Data collection was realized on November 1, 2023 at the Ostrava site and on March 15, 2024 at the Girova Area of interest (AOI). Basic information about the image acquisition is provided in **Table 1**.

All flights were realized in automatic mode via the DJI Pilot app. At both sites, a flight with active GNSS RTK positioning was first performed, immediately followed by a second flight according to an identical flight mission, but with only a standard GNSS receiver. In area Ostrava, only nadiral images were acquired. In the mountainous area Girova, nadiral images were complemented with a set of side-looking (oblique) images from a manual flight to improve quality of model reconstruction. Weather conditions were good, with minimal wind and stable lighting.

To enable accurate indirect georeferencing of products derived from image sets captured using only a standard GNSS receiver, and to allow for an independent comparison of both approaches (direct and indirect georeferencing), a set of ground control points (GCPs) was temporarily signalized in both areas of interest (AOIs). A total of 20 GCPs were established in the Girova area, and 25 GCPs in the Ostrava area. Their positions were measured using a geodetic-grade Trimble R10 GNSS receiver operating in RTK mode.

At the Ostrava site, the RTK solution was obtained by connecting to the nearest GNSS reference station, located just 1.6 km from the AOI. In Girova, the network RTK service provided by the commercial GNSS reference station network TopNET was used. As the closest physical reference station is approximately 25 km away, the network-based solution was employed to ensure higher positioning accuracy. The same RTK correction sources were used by the DJI Mavic 3 Enterprise UAV during image acquisition at both sites.

In Ostrava, GCPs were evenly distributed across the entire area, including all corners and the central region. In Girova, a uniform distribution of GCPs was not possible due to challenging topography and vegetation, which in some locations prevented fixed RTK positioning. Therefore, the GCPs were positioned to maximize area coverage and include all elevation levels under the given constraints. As described below, part of the GCPs was used for georeferencing during processing, while the remaining points were used to evaluate the positional accuracy of the derived products.

Table 1.

Flight and imaging parameters by area.

Parameter	Ostrava	Girova
Average height of flight	60 m	70 m
Average ground sample distance (GSD)	1.6 cm	1.9 cm
Front, side image overlap	80%, 80%	85%, 85%
Number of images	328 (RTK mode), 324 (standard mode)	211 (RTK mode), 210 (standard mode)

2.3. Image processing

Image processing was carried out using Agisoft Metashape Professional software v.2.1.3 (https://www.agisoft.com/). Identical workflow and parameters settings was applied to process all four sets of images. The only difference was in georeferencing the products which was based either on a set of GCPs (non-RTK datasets) or directly on position of images estimated by drone's own RTK receiver (RTK datasets).

In the initial stage of the workflow, images in the raw DGN file format were imported into the software and aligned using accuracy settings on High with a key points limit of 40,000 and a tie points limit of 10,000. This configuration ensured robust feature matching across overlapping images, yielding a reliable sparse point cloud as the foundation for subsequent analyses.

For the non-RTK datasets, a georeferencing procedure incorporating GCPs was implemented. For AOI Ostrava, 11 GCPs were utilized in the processing stage, with 14 GCPs designated for accuracy validation. Similarly, For AOI Girova, a total of 9 GCPs were used for georeferencing, while an additional 11 GCPs were reserved for independent accuracy assessment. The selection of GCPs used for georeferencing was evenly distributed across both study areas to ensure comprehensive spatial coverage. GCPs were imported into the project, and corresponding markers were manually placed across all the relevant images. Georeferencing including camera optimization was performed

using the GCPs data. In contrast, the RTK datasets benefitted from the pre-embedded high-precision camera location data, allowing the workflow to focus solely on optimizing the camera alignment based on these coordinates without the time-consuming manual work with GCPs. In both RTK and non-RTK modes, the calibration parameters—including the focal length (f), affinity and non-orthogonality coefficients (b1 and b2), principal point coordinates (cx and cy), radial distortion coefficients (k1 through k4), and tangential distortion coefficients (p1 and p2)—were optimized.

After georeferencing, depth maps were generated using quality settings on High combined with aggressive filtering. These depth maps served as the basis for constructing a dense point cloud, which in turn was used to generate a raster Digital Elevation Model (DEM). The DEM then provided the reference surface for the orthophoto mosaic creation process; notably, hole filling was disabled during orthophoto mosaic generation to preserve the integrity of the raw data. Throughout all processing steps, the WGS-84 coordinate system was employed to ensure consistency across all derived products. Additionally, all other processing settings, including image alignment, point cloud generation, digital elevation model (DEM) creation, and orthophoto mosaic production, were kept identical for both study areas. This standardized approach was essential to maintaining consistency across datasets and ensuring a fair comparison between RTK and non-RTK results.

The final outputs, including the DEM and orthophoto mosaic, were generated for both the Ostrava and Girova areas of interest using RTK and non-RTK workflows. For the Ostrava area, the DEM has a spatial resolution of 3.16 cm/pixel, while the orthophoto mosaic has a resolution of 1.58 cm/pixel. For the Girova area, the DEM resolution is 3.76 cm/pixel, and the orthophoto mosaic resolution is 1.88 cm/pixel. These datasets were then exported for further comparative analysis.

2.4. Accuracy Assessment

A set of GCPs that were not incorporated into the image processing stage was employed as independent validation markers. Elevation values corresponding to the horizontal position of these GCPs were extracted from the generated DEMs. Differences between the elevation of GCPs and the corresponding extracted DEM values were computed, thus quantifying the vertical discrepancies between the field measurements and the modelled data. Specifically, for each point i, the error is defined as:

$$e_i = Z_i^{DEM} - Z_i^{GCP} \tag{1}$$

where Z_i^{DEM} is the elevation extracted from the DEM and Z_i^{GCP} is the GCP elevation.

These differences were subsequently analyzed using a range of statistical measures, including the mean error to gauge overall bias, standard deviation or the root mean square error (RMSE) as shown below.

$$\text{Mean of Errors (ME)} = \frac{1}{n}\sum_{i=1}^{n} e_i \tag{2}$$

$$Standard\ Deviation\ of\ Errors\ \ (SDEV) = \sqrt{\frac{1}{n-1}\sum_{i=1}^{n}(e_i - ME)^2} \tag{3}$$

$$Root\ Mean\ Square\ Error\ (RMSE) = \sqrt{\frac{1}{n}\sum_{i=1}^{n} e_i^2} \tag{4}$$

The evaluation of the horizontal accuracy was realized on the orthophoto mosaics. Differences in the X (longitude) and Y (latitude) coordinates between the centers of GCP targets on the orthophoto mosaics and their position obtained by field measurement were computed. To integrate the individual coordinate differences into a single measure of positional accuracy, the Haversine formula was applied to compute the horizontal distance. The haversine formula, which calculates the great-circle distance based on latitude and longitude is expressed as:

$$a = sin^2\left(\frac{\Delta\varphi}{2}\right) + \cos(\varphi_1)cos(\varphi_2)sin^2\left(\frac{\Delta\lambda}{2}\right) \quad (5)$$

$$c = 2.atan2\left(\sqrt{a}, \sqrt{(1-a)}\right) \quad (6)$$

$$d = R.c \quad (7)$$

where φ_1 and φ_2 are the latitudes

$\Delta\varphi$ and $\Delta\lambda$ are the differences in latitude and longitude (in radians)

R is the Earth's radius (approximately 6,371 km), (Sinnott, 1984).

The resulting latitude and longitude errors, as well as the derived horizontal distance, were again analyzed statistically.

3. RESULTS

Table 2 summarizes the elevation accuracy statistics for the DEMs derived from both RTK and non-RTK datasets in the two areas of interest. All statistical parameters fall within expected ranges, not exceeding a few centimeters. However, the results indicate that the mean error was significantly higher for datasets produced using direct georeferencing compared to those produced using indirect georeferencing in both Ostrava and the Girova AOI. In terms of standard deviation, both approaches yielded similar results, with a difference of only about 0.5 cm. The standard deviation values were notably higher in the Girova AOI, which can be attributed to the complex topography and the relatively large distance to the nearest GNSS reference station.

Table 2.

DTM accuracy statistics (vertical error) statistics in cm.

	Ostrava AOI		**Girova AOI**	
	RTK	Non-RTK	RTK	Non-RTK
ME	-6.47	-1.15	2.28	0.30
SDEV	0.88	1.46	3.80	3.33
RMSE	6.52	1.82	4.28	3.19

More detailed results at the level of individual control points are presented in **Fig. 3** for Ostrava and in **Fig. 4** for Girova, along with the corresponding DEMs illustrating the topography of each area of interest. The results from Ostrava reveal a clear systematic error in the DEM heights derived from the RTK-based dataset, as all control points exhibit a similar negative vertical offset. This may be attributed to an error in determining the focal length of the camera during photogrammetric processing under direct georeferencing, as documented by Štroner et al. (2021).

In contrast, this issue did not appear in the Girova AOI, likely due to the inclusion of both nadir and oblique images in the dataset. The effectiveness of combining image perspectives to improve model accuracy has also been confirmed by Štroner et al. (2021). Aside from the observed systematic bias in Ostrava, there is no distinct spatial pattern in the error distribution across individual control points. In the Ostrava AOI, none of the points showed anomalous behavior relative to the rest.

In the Girova AOI, the maximum error was observed at control point no. 11, located in the eastern part of the area at the top of the landslide. The error at this point reached 12.18 cm in the RTK-based dataset and 6.76 cm in the non-RTK dataset. In the latter case, two GCPs used for georeferencing were located within approximately 30 meters of this control point, which likely contributed to improved DEM accuracy in this part of the AOI. Nevertheless, the elevated error at point no. 11 may also have been influenced by inaccuracies in the vertical positioning of the point itself.

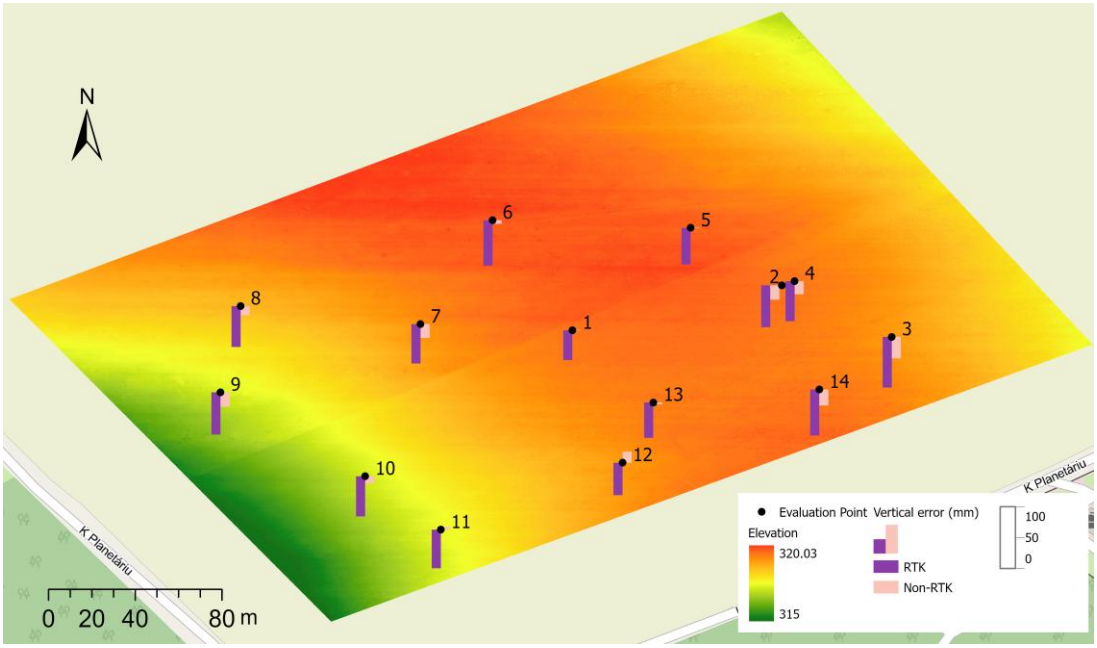

Fig. 3. Vertical error of individual control points in the Ostrava AOI from RTK and Non-RTK datasets shown on top of the DEM. Source of background map: Open Street Map.

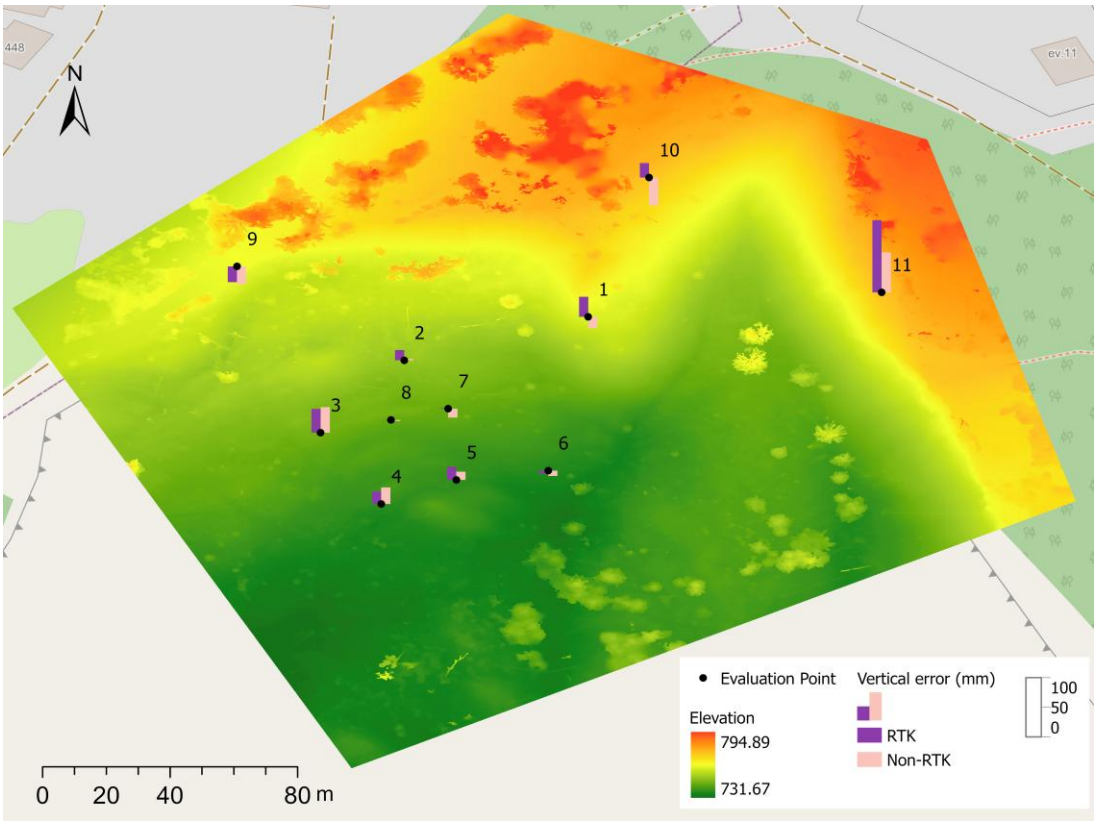

Fig. 4. Vertical error of individual control points in the Girova AOI from RTK and Non-RTK datasets shown on top of the DEM. Source of background map: Open Street Map.

Table 3 presents the statistics for the latitude and longitude differences between position of GCPs measured in the field and derived from orthophoto mosaics, as well as the statistics for their distances. The horizontal accuracy assessment of the orthophoto mosaics for the Ostrava AOI reveals small differences between the RTK and non-RTK datasets. For the RTK data, the mean errors were –1.31 cm in longitude and –0.66 cm in latitude, resulting in a mean horizontal distance error of 3.75 cm. The standard deviation was 1.50 cm for the distance error, while the RMSE 4.02 cm, respectively. In comparison, the non-RTK dataset exhibited slightly larger values with mean horizontal distance error of 4.74 cm, standard deviation of 2.60 cm and the RMSE of 5.36 cm, respectively. Nevertheless, both approaches led to similar results with expectable statistics reaching a few centimeters level. The horizontal accuracy assessment for the orthophoto mosaics in the Girova AOI are also summarized in **Table 3**. For the RTK (non-RTK) dataset, the mean horizontal distance error was 3.75 cm (3.34 cm), standard deviation computed from distances of 1.83 cm (1.48 cm) and RMSE computed from distances of 4.13 cm (3.63 cm). The results of the two approaches are again comparable, with slightly lower values of statistical parameters this time achieved by the georeferencing based on GCPs.

Table 3.

Horizontal error statistics in cm.

	Ostrava AOI						**Girova AOI**					
	RTK			**Non-RTK**			**RTK**			**Non-RTK**		
	Long error	Lat error	Dist	Long error	Lat error	Dist	Long error	Lat error	Dist	Long error	Lat error	Dist
ME	-1.31	-0.66	3.75	-2.56	2.83	4.74	1.97	-0.9	3.75	-1.27	-0.31	3.34
SDEV	3.18	3.29	1.5	2.69	3.88	2.6	2.22	3.3	1.83	2.19	3.05	1.48
RMSE	3.33	3.24	4.02	3.65	4.69	5.36	2.89	3.27	4.13	2.44	2.93	3.63

Latitude and longitude errors at individual control points are presented in **Fig. 5** for the Ostrava AOI and in **Fig. 6** for the Girova AOI, respectively.

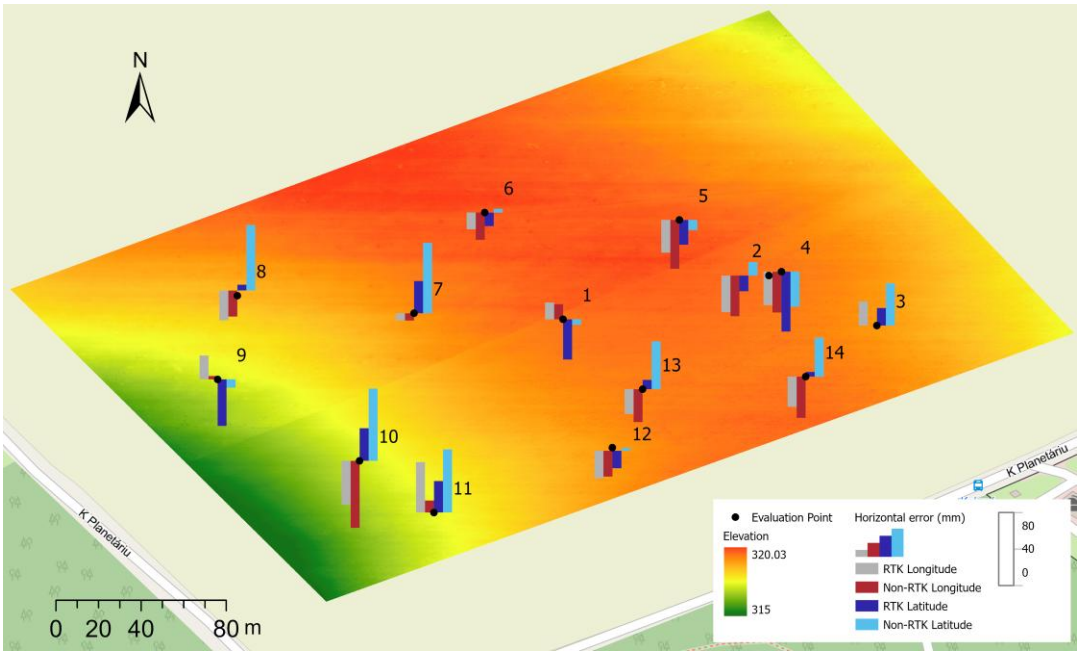

Fig. 5. Horizontal (latitude, longitude) errors of individual control points in the Ostrava AOI from RTK and Non-RTK datasets shown on top of the DEM. Source of background map: Open Street Map.

In Ostrava, there is no clear systematic pattern observable across the entire area, nor does any single control point exhibit significantly different behavior compared to the others. However, some local groupings with similar error characteristics can be identified.

Specifically, control points no. 7, 8, 10, and 11, located in the western part of the Ostrava AOI, showed similarly elevated latitude errors in the non-RTK dataset. Conversely, in the eastern part of the AOI, points no. 2, 4, 5, and 14 exhibited similar longitude errors in both RTK and non-RTK datasets. These observations suggest that the spatial distribution of horizontal errors in the Ostrava AOI is not entirely random and may reflect localized effects, possibly related to image geometry or processing parameters.

In contrast, horizontal error values in the Girova AOI appear to be randomly distributed. No systematic spatial patterns are visible across the entire area or within any sub-regions, regardless of whether direct or indirect georeferencing was applied. Interestingly, control point no. 11, which exhibited the highest vertical error, was among the points with the lowest horizontal errors in Girova, with latitude and longitude errors around 2 cm.

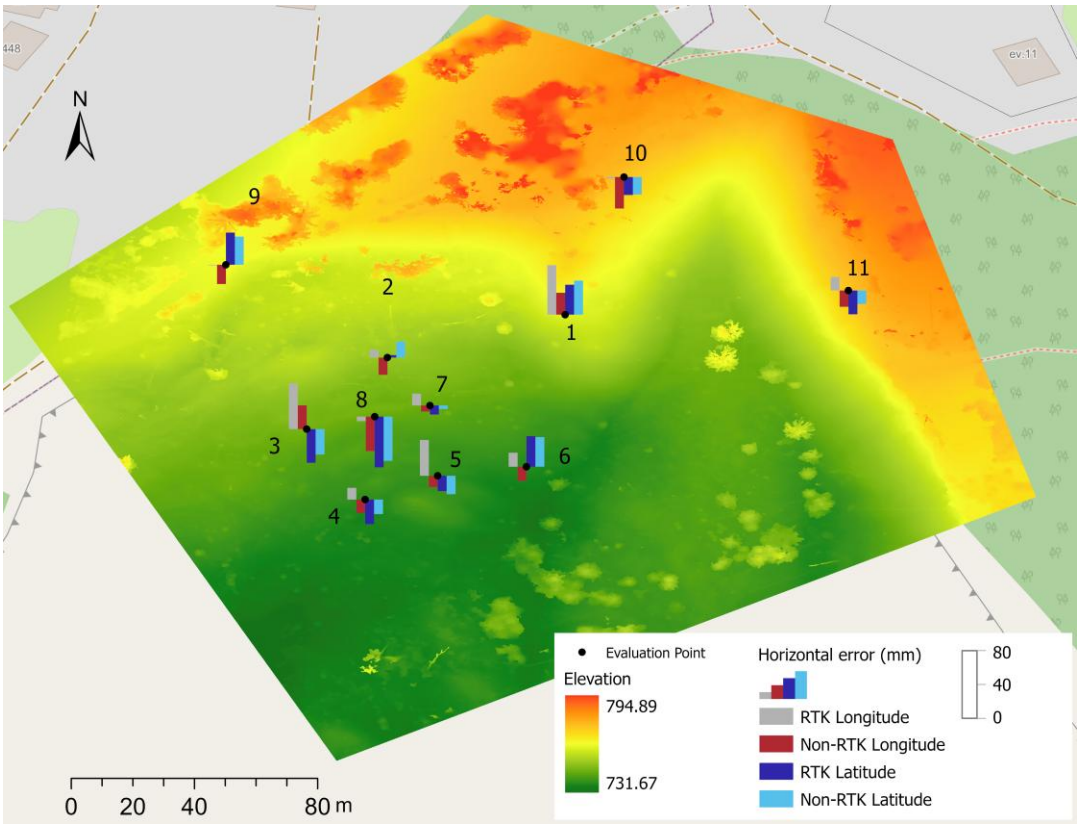

Fig. 6. Horizontal (latitude, longitude) errors of individual control points in the Girova AOI from RTK and Non-RTK datasets shown on top of the DEM. Source of background map: Open Street Map.

4. DISCUSSION AND CONCLUSION

This study provides a comparative assessment of direct and indirect georeferencing methods in UAV-based mapping across two contrasting landscapes. UAV surveys were conducted using a DJI Mavic 3 Enterprise quadcopter equipped with an RTK module at two sites in the Czech Republic: a flat agricultural area near Ostrava and a mountainous region with complex topography in the Girova area of the Silesian Beskydy Mountains. From these surveys, DEMs and orthophoto mosaics were

generated through photogrammetric processing and subsequently analyzed to evaluate the accuracy of each georeferencing approach under varying terrain conditions. The comparison was based on horizontal and vertical error measurements relative to control reference points.

In general, both georeferencing techniques provided the expected level of accuracy for DEMs and orthophoto mosaics, typically within a few centimeters. However, some differences between the methods were observed. The results indicate that indirect georeferencing using ground control points (GCPs) yielded slightly better vertical accuracy compared to direct georeferencing with RTK. DEMs generated from non-RTK workflows exhibited lower RMSE values and no apparent systematic errors across both areas of interest, suggesting that RTK-based direct georeferencing did not significantly improve vertical accuracy under the given conditions. These findings are consistent with those of Martínez-Carricondo et al. (2023), who reported improved accuracy using GCPs, and with Przybilla et al. (2020) and Štroner et al. (2021), who showed that the absence of GCPs can lead to substantial systematic height deviations—up to 30 times the ground sampling distance (GSD). However, this observation contrasts with the results of Tomaštík et al. (2019), who demonstrated that UAV-RTK systems can achieve vertical accuracies comparable to workflows using nine GCPs, and significantly better than those using only four GCPs. It is worth noting that their study was conducted over a large and complex area of 270 hectares, where the number of GCPs may have been insufficient for optimal georeferencing. Additionally, differences in UAV platforms may have contributed to the varying results. The studies reporting better performance with GCPs all used the DJI Phantom 4 RTK quadcopter, whereas Tomaštík et al. (2019) employed the more advanced fixed-wing SenseFly eBee Plus, which may offer enhanced flight stability and positioning capabilities.

For horizontal accuracy, the results varied between the two areas of interest. In Ostrava, direct georeferencing (RTK) yielded slightly better accuracy than the GCP-based approach, while in Girova, the opposite was observed. These findings are consistent with the conclusions of Szypuła (2024) and Elias et al. (2024), who emphasized that the use of GCPs enhances positional accuracy, particularly in complex terrain. Nevertheless, the differences in horizontal accuracy between the two georeferencing methods in this study were minimal, with discrepancies in the reported statistical parameters generally below or around 1 cm.

The quality of GNSS differential positioning, including RTK and PPK techniques, is influenced by the length of the baseline—defined as the distance between the reference station providing corrections and the rover receiver used to determine the coordinates of measured objects. As baseline length increases, positioning accuracy generally decreases. To maintain high accuracy over longer baselines, network RTK solutions are typically employed, which combine observations from multiple reference stations or from an entire reference station network. As described in Section 2.2, a direct connection to a nearby GNSS reference station was used in the Ostrava AOI, while a network RTK solution was applied in the Girova AOI for both UAV image acquisition and ground control point positioning. The DJI Mavic 3 Enterprise quadcopter automatically records a file containing the formal RTK positioning errors (i.e., standard deviations of the estimated positioning errors) for each captured image. In the Ostrava AOI, the mean formal RTK positioning errors recorded by the UAV were 1.1 cm in latitude, 0.8 cm in longitude, and 1.8 cm in height. In contrast, the corresponding values in the Girova AOI were 1.8 cm in latitude, 1.2 cm in longitude, and 3.1 cm in height. The lower error values in Ostrava can be attributed to the much shorter baseline, as opposed to the Girova site, where the nearest physical reference station in the network solution was approximately 25 km away. Nevertheless, these differences in formal positioning errors did not appear to significantly affect the georeferencing quality of the resulting orthophoto mosaics and digital elevation models (DEMs).

This study reinforces previous research findings that GCPs remain essential for achieving optimal georeferencing accuracy, particularly in the vertical (height) component. However, in scenarios where rapid deployment and operational efficiency are prioritized, RTK enabled UAVs offer a viable alternative. The effectiveness of RTK positioning relies on phase measurements with fixed integer ambiguities, making it suitable primarily for environments with unobstructed sky visibility. Temporary or permanent obstructions between the GNSS receiver and satellites such as vegetation, buildings, or steep terrain can significantly degrade positioning accuracy. These limitations are

generally not relevant during UAV based image acquisition, as the UAV typically operates above such obstacles. In this context, our review of scientific literature did not identify any reported stability issues of UAV mounted RTK systems related to these obstructions. Conversely, such obstacles can present challenges for the precise positioning of GCPs or may restrict their deployment within the area of interest. Another potential limitation of RTK is its reliance on a stable internet connection for receiving real time correction data. Limited mobile network coverage can impair both UAV data acquisition and ground based GCP measurements. In areas lacking sufficient connectivity, alternative techniques such as PPK positioning must be employed.

Future research should explore hybrid approaches that integrate RTK with a minimal set of GCPs to balance efficiency and accuracy. This approach was suggested, for example, by Benassi et al. (2017) and has proven effective in various applications, as demonstrated by Przybilla et al. (2020) and Elias et al. (2024). In addition, future studies should consider expanding into more diverse and operationally challenging terrains, such as urban canyons or forested ridges, to better assess RTK performance under conditions where signal degradation, multipath errors, and occlusions are more prevalent. Such environments would offer further insight into the robustness and practical limitations of RTK-based workflows.

ACKNOWLEDGEMENT

This work was partially supported by Grant of SGS No. SP2025/040, Faculty of Mining and Geology, VSB - Technical University Ostrava.

REFERENCES

Atik, M. E., & Arkali, M. (2025). Comparative Assessment of the Effect of Positioning Techniques and Ground Control Point Distribution Models on the Accuracy of UAV-Based Photogrammetric Production. Drones, 9(1). https://doi.org/10.3390/drones9010015.

Baroň, I., Řehánek, T., Vošmik, J., Musel, V., & Kondrová, L. (2011). Report on a recent deep-seated landslide at Gírová Mt., Czech Republic, triggered by a heavy rainfall: The Gírová Mt., Outer West Carpathians; Czech Republic. Landslides, 8(3), 355–361. https://doi.org/10.1007/s10346-011-0255-y.

Benassi, F., Dall'Asta, E., Diotri, F., Forlani, G., di Cella, U.M., Roncella, R., Santise, M. (2017). Testing accuracy and repeatability of UAV blocks oriented with gnss-supported aerial triangulation. Remote Sensing, 9, 172. https://doi.org/10.3390/rs9020172.

Colomina, I., Blázquez, M., Molina, P., Parés, M. E., & Wis, M. (2008). Towards a new paradigm for high-resolution low-cost photogrammetry and remote sensing. Int. Archives of Photogrammetry, Remote Sensing and Spatial Information Sciences, Beijing, China, 37(B1), 1201–1206.

Colomina, I., & Molina, P. (2014). Unmanned aerial systems for photogrammetry and remote sensing: A review. In ISPRS Journal of Photogrammetry and Remote Sensing (Vol. 92, pp. 79–97). Elsevier B.V. https://doi.org/10.1016/j.isprsjprs.2014.02.013.

Cromwell, C., Giampaolo, J., Hupy, J., Miller, Z., & Chandrasekaran, A. (2021). A systematic review of best practices for uas data collection in forestry-related applications. In Forests (Vol. 12, Issue 7). MDPI AG. https://doi.org/10.3390/f12070957.

Czyża, S., Szuniewicz, K., Kowalczyk, K., Dumalski, A., Ogrodniczak, M., & Zieleniewicz, Ł. (2023). Assessment of Accuracy in Unmanned Aerial Vehicle (UAV) Pose Estimation with the REAL-Time Kinematic (RTK) Method on the Example of DJI Matrice 300 RTK. Sensors, 23(4). https://doi.org/10.3390/s23042092.

Elias, M., Isfort, S., Eltner, A., & Maas, H. G. (2024). UAS Photogrammetry for Precise Digital Elevation Models of Complex Topography: A Strategy Guide. ISPRS Annals of the Photogrammetry, Remote Sensing and Spatial Information Sciences, 10(2), 57–64. https://doi.org/10.5194/isprs-annals-X-2-2024-57-2024.

Gomez, C., & Purdie, H. (2016). UAV- based Photogrammetry and Geocomputing for Hazards and Disaster Risk Monitoring – A Review. In Geoenvironmental Disasters (Vol. 3, Issue 1). Springer. https://doi.org/10.1186/s40677-016-0060-y.

Martínez-Carricondo, P., Agüera-Vega, F., & Carvajal-Ramírez, F. (2023). Accuracy assessment of RTK/PPK UAV-photogrammetry projects using differential corrections from multiple GNSS fixed base stations. Geocarto International, 38(1). https://doi.org/10.1080/10106049.2023.2197507.

Mohsan, S. A. H., Khan, M. A., Noor, F., Ullah, I., & Alsharif, M. H. (2022). Towards the Unmanned Aerial Vehicles (UAVs): A Comprehensive Review. In Drones (Vol. 6, Issue 6). Multidisciplinary Digital Publishing Institute (MDPI). https://doi.org/10.3390/drones6060147.

Nakata, Y., Iwasaki, K., Shimoda, S., & Torita, H. (2023). Understanding microtopography changes in agricultural landscapes through precision assessments of digital surface models by the UAV-RTK-PPK method without ground control points. Smart Agricultural Technology, 5. https://doi.org/10.1016/j.atech.2023.100269.

Nam-Bui, X., Quoc Long, N., Thi Thu Ha, L., Ngoc Quy, B., Goyal, R., Trong Hung, V., van Chung, P., Xuan Cuong, C., van Canh, L., & Hong Viet, L. (2020). Flight Height of UAV and Its Influence on the Precise Digital Elevation Model of Complex Terrain. Inzynieria Mineralna, 2020(1), 179–186. https://doi.org/10.29227/IM-2020-01-27.

Przybilla, H. J., Bäumker, M., Luhmann, T., Hastedt, H., & Eilers, M. (2020). Interaction between direct georeferencing, control point configuration and camera self-calibration for RTK-based UAV photogrammetry. International Archives of the Photogrammetry, Remote Sensing and Spatial Information Sciences - ISPRS Archives, 43(B1), 485–492. https://doi.org/10.5194/isprs-archives-XLIII-B1-2020-485-2020.

Rauhala, A., Meriö, L. J., Kuzmin, A., Korpelainen, P., Ala-Aho, P., Kumpula, T., Kløve, B., & Marttila, H. (2023). Measuring the spatiotemporal variability in snow depth in subarctic environments using UASs - Part 1: Measurements, processing, and accuracy assessment. Cryosphere, 17(10), 4343–4362. https://doi.org/10.5194/tc-17-4343-2023.

Sinnott, R. W. (1984). Virtues of the haversine. Sky and Telescope, 68(2), 159.

Stott, E., Williams, R. D., & Hoey, T. B. (2020). Ground control point distribution for accurate kilometre-scale topographic mapping using an rtk-gnss unmanned aerial vehicle and sfm photogrammetry. Drones, 4(3), 1–21. https://doi.org/10.3390/drones4030055.

Štroner, M., Urban, R., Seidl, J., Reindl, T., & Brouček, J. (2021). Photogrammetry using UAV-mounted GNSS RTK: Georeferencing strategies without GCPs. Remote Sensing, 13(7). https://doi.org/10.3390/rs13071336

Szypuła, B. (2024). Accuracy of UAV-based DEMs without ground control points. GeoInformatica, 28(1), 1–28. https://doi.org/10.1007/s10707-023-00498-1.

Teunissen, P.J.G., Montenbruck, O. (eds.) (2017). Springer Handbook of Global Navigation Satellite Systems. Springer International Publishing. ISBN 978-3-319-42926-7. doi:10.1007/978-3-319-42928-1.

Tomaštík, J., Mokroš, M., Surový, P., Grznárová, A., & Merganič, J. (2019). UAV RTK/PPK method-An optimal solution for mapping inaccessible forested areas? Remote Sensing, 11(6). https://doi.org/10.3390/RS11060721.